Solar neutrino data and their implications

Evalyn Gates,* Lawrence Krauss,† and Martin White‡
Center for Theoretical Physics, Sloane Laboratory, Yale University, New Haven, Connecticut 06511
(Received 5 March 1992)

The complete and concurrent Homestake and Kamiokande solar neutrino data sets (including backgrounds), when compared to detailed model predictions, provide no unambiguous indication of the solution to the solar neutrino problem. All neutrino-based solutions, including time-varying models, provide reasonable fits to both the 3-yr concurrent data and the full 20-yr data set. A simple constant B neutrino flux reduction from the standard solar model mean prediction is ruled out at greater than the 4σ level for both data sets. While such a flux reduction provides a marginal fit to the unweighted averages of the concurrent data, it does not provide a good fit to the average of the full 20-yr sample. Gallium experiments may not be able to distinguish between the currently allowed neutrino-based possibilities.

PACS number(s): 96.60.Kx, 14.60.Gh

I. INTRODUCTION

Perhaps at no time in the past 20 years has there been more interest in the solar neutrino problem than at the present moment. The apparent deficit of high-energy solar neutrinos observed by the Homestake Solar Neutrino Detector over two decades [1] has now been confirmed by the Kamiokande large underground water Cherenkov detector [2]. Gallium detectors are beginning to come on line and the Soviet-American Gallium Experiment (SAGE) group has recently published their first results [3], which seem to indicate a neutrino deficit that cannot be explained by solar physics (for a brief discussion see [4]). Other detectors are approved or are in the planning stages, and there is hope that a solution to the solar neutrino problem may be at hand. At the same time a growing number of theoretical neutrino-based "solutions" have been proposed. Heading the list appears to be the Mikheyev-Smirnov-Wolfenstein (MSW) solution [5,6], which, in a restricted but reasonable range of neutrino masses and mixing angles, allows significant reduction in the neutrino signal to be observed. An alternative solution involves a large neutrino magnetic moment, either diagonal or transitional, which causes neutrinos to oscillate into "sterile" partners while traversing the magnetic field of the Sun [7,8]. While this seems less theoretically compelling, especially in view of the large neutrino magnetic moments required, it has the distinct advantage of allowing not only the neutrino signal to be time varying over the solar cycle, but also allows for a different time variation to be observed in different detectors [9].

It may seem *a priori* that the simplest solution of the original Cl solar neutrino problem resides in the solar model itself, namely that fewer high-energy neutrinos are created in the Sun than the standard solar model suggests. It is important to determine if this possibility can be ruled out, although it seems increasingly difficult to accommodate, especially in light of the new SAGE results [3]. Also, astrophysical mechanisms which reduce the high-energy neutrino flux are now not supported by any other solar measurements (most importantly the *p*-mode fine structure [10,1]). Meanwhile, several studies incorporating recent Cl data into the 20-yr observations provide very tempting, if not compelling, evidence of time variations in the Cl signal [11–13] which may be correlated, in some yet to be determined way, with the solar cycle. On the other hand, the Kamiokande data appear naively to show no such time variation. The presence, for the first time, of two different data sets for the solar neutrino signal should allow a number of finer tests of solar neutrino models to be made (see, e.g., [2]). Surprisingly, however, rarely have all the data been observed. For example, analyses have been performed comparing the Homestake 20-yr "average" signal with the averaged Kamiokande 3-yr signal. It is not clear that such a procedure is correct. Until we have a better idea of what is at the root of the solar neutrino problem, we can make no *a priori* claims about what the Kamiokande signal would have been if the detector had also taken data during the 20 years Homestake was operational, especially given the apparent variations in the Cl data during this period. All of the data points from both experiments should be exploited, and the error bars examined. For guidance on how to treat the entire data sets one can first analyze the data during the period in which the two detectors were both running concurrently. It is only during this time that we have a direct independent check on the Cl data, and can check for consistency between the data sets. One might then be guided on how to use all the data to test various hypotheses. This is the spirit of the

*Address after October 1, 1992: Department of Physics, University of Chicago.
†Also at the Department of Astronomy. Electronic address: krauss@yalehep.
‡Address after September 1, 1992: Center for Particle Astrophysics, University of California, Berkeley.

following work. We have utilized the entire Homestake and Kamiokande data sets, concentrating first on the concurrent data sets and then on all the data, in order to investigate the range of models which may or may not fit the data. We have carried out extensive numerical model calculations, in which neutrinos are propagated, with complete phase information, through much of the Sun, in order to estimate the flux in various neutrino species at the Earth's surface. We have also used realistic models of detector sensitivity in order to turn fluxes into detection rates.

We emphasize that using the concurrent Kamiokande data to "check" the Cl data is important beyond the strict question of whether or not any solar cycle time variation exists. It allows us to understand how best to treat the full 20-yr Cl data to explore solutions to the solar neutrino problem. We display in Fig. 1(a) and (b) the two full data sets, and the concurrent data sets (see Sec. III for a fuller discussion of the data sets). Both data sets are normalized to the mean standard solar model (SSM) [1] predictions.

While quoted averages of the two data sets appear at first sight to differ, when the full data sets are displayed this issue is less clear. The Cl signal clearly has much more jitter, with several apparently anomalously low points, but aside from this one might not be surprised if told that all data came from a single detector. This may suggest that a simple, energy-independent deficit of B neutrinos could be consistent with all of the data. To properly explore this possibility, as well as the possibility that the solar neutrino deficit is neutrino related, a more quantitative approach is required.

In the following we incorporate fluxes based on the predictions of the standard solar model, without "uncertainties," which we refer to as the SSM. This point should be kept in mind when interpreting the confidence levels quoted later. We expect that including these uncertainties will not be likely to dramatically alter our results. Most of the SSM uncertainty is associated with the boron neutrino flux which will be strongly suppressed in models which fit the data. Thus the effect of this uncertainty is minimized. The main effect of including the errors will be to broaden somewhat the range of model parameters allowed in our confidence level regions, and also to broaden the range of "best-fit" parameters. The most important point is that including these uncertainties will not be likely to affect the overall consistency of model fits to the data. Those models which do not provide good fits to the data before considering uncertainties will not be likely to do so afterwards. (We have graphically demonstrated this by considering solar model uncertainties in work that was submitted for publication after this manuscript was submitted but before it went to press [14].)

II. NEUTRINO FLUX AT THE EARTH

The neutrino spectrum predicted by the standard solar model (SSM) is described in detail by Bahcall in [1]. The dominant neutrino flux, that due to the *pp* reaction in the Sun, with energies less than 0.42 MeV, is unobservable in both the Cl and Kamiokande detectors, due to their thresholds. The component of the flux which gives the dominant contribution to the Cl signal, and the entire contribution to Kamiokande, is the high energy ^{8}B continuous spectrum ($^8\mathrm{B}\rightarrow{}^7\mathrm{Be}^*+e^++\nu_e$), with neutrino energies up to 15 MeV and a total predicted flux at the Earth of $(5.8\pm2.2)\times10^6\ \mathrm{cm}^{-2}\mathrm{s}^{-1}$ ("3σ" theoretical error). The only other components of the neutrino spectrum contributing to the Cl signal at greater than the 5% level are the Be neutrinos ($^7\mathrm{Be}+e^-\rightarrow{}^7\mathrm{Li}+\nu_e$), with fixed energy 0.862 MeV and a predicted flux of $4.7\pm0.7(3\sigma)\times10^9\ \mathrm{cm}^{-2}\mathrm{s}^{-1}$.

There are two ways one might expect to alter these predicted fluxes. First one might lower the overall flux by a fixed amount by postulating some new solar physics. For example, if the core temperature is lowered compared to the SSM, the B signal can be significantly reduced (such a temperature reduction is the aim of many nonstandard solar models, e.g., see [1]).

We have incorporated these possibilities in our analysis by treating the net B flux as a free parameter in one set of runs, and examining the goodness of fit with the combined data sets as this parameter is varied compared to the SSM. While this is a very simplistic "nonstandard solar model" we can use it to perform straightforward statistical tests of how well the data is fit by models aiming at such a B flux reduction.

The other possibility is that the origin of the solar neutrino problem lies in the properties of neutrinos themselves. If neutrinos have nonzero mass eigenstates which do not coincide with weak eigenstates, neutrino propagation will lead to oscillations between the different weak states, namely between electron, muon, and tau neutrinos. Since the Cl detector is sensitive *only* to electron neutrinos, while the Kamiokande water detector is sensitive *predominantly* to electron neutrinos, such oscillations could have the possibility of reducing the observed signal in both detectors [25]. Moreover, the presence of matter can enhance the oscillations between neutrino species [5] due to the presence of level crossings which occur as the background electron density varies. If one supplements neutrino masses with large magnetic moments, which in general need not be diagonal in the weak basis, then another possibility arises. Magnetic fields in the Sun could cause oscillations between left- and right-handed neutrino states, with or without induced level crossings [7]. In general, left-right mixing can allow neutrino states to oscillate into antineutrino states, unlike the pure MSW mechanisms [8]. In any case, as long as the right-handed states have suppressed interaction rates in the detectors, this can reduce the observed neutrino signal. Moreover, it allows for a possible correlation with the solar cycle, although the required neutrino magnetic moments, at least for currently envisaged magnetic field strengths in the Sun, are large enough to cause other potential astrophysical problems [15]. Finally, in the most general case, both effects may be operational with the different factors dominating in different regimes of mass, mixing angle, and magnetic field space [8]. This allows independent time variations to be observed in the two

detectors [9], and it is this general case which we shall consider here.

We followed explicitly the propagation of neutrinos through the Sun by numerically integrating the Hamiltonian evolution equation for neutrinos through matter for a two-generation model with Majorana-type transition magnetic moment and off-diagonal mass terms [8,9,16,17]:

$$i\frac{d}{dt}\begin{bmatrix}\nu_e\\ \nu_\mu\\ \bar{\nu}_e\\ \bar{\nu}_\mu\end{bmatrix}=H\begin{bmatrix}\nu_e\\ \nu_\mu\\ \bar{\nu}_e\\ \bar{\nu}_\mu\end{bmatrix}. \tag{1}$$

The Hamiltonian for the system [8] is given by

$$H=\begin{bmatrix} a_e & \frac{\Delta m^2}{4E_\nu}\sin 2\theta & 0 & \mu B \\ \frac{\Delta m^2}{4E_\nu}\sin 2\theta & \frac{\Delta m^2}{2E_\nu}\cos 2\theta + a_\mu & -\mu B & 0 \\ 0 & -\mu B & -a_e & \frac{\Delta m^2}{4E_\nu}\sin 2\theta \\ \mu B & 0 & \frac{\Delta m^2}{4E_\nu}\sin 2\theta & \frac{\Delta m^2}{2E_\nu}\cos 2\theta - a_\mu \end{bmatrix} \tag{2}$$

where B is the magnetic field, $a_e = G_F(2N_e - N_n)/\sqrt{2}$ and $a_\mu = G_F(-N_n)/\sqrt{2}$ with N_e, N_n the electron and neutron densities as a function of radius in the solar interior. We used the following fit to the electron and neutron densities in the standard model sun [1]:

$$N_e = \begin{cases} 2.45\times 10^{26}\exp(-10.54x), & x > 0.2\ , \\ 6\times 10^{25}[1-10x/3]/\mathrm{cm}^3, & x < 0.2, \end{cases} \tag{3}$$

$$N_n = \begin{cases} 2.45\times 10^{26}\exp(-10.54x), & x > 0.2\ , \\ 2\times 10^{25}[1-21x/5]/\mathrm{cm}^3, & x < 0.2, \end{cases} \tag{4}$$

where $x = r/R_\odot$.

The free parameters in the calculations are the neutrino energy E, mass-squared difference Δm^2, vacuum mixing angle $\sin^2(2\theta)$, and Zeeman energy μB: the product of the transition magnetic moment and solar magnetic field. For reasons of simplicity we assumed this to be uniform over the radiation and convection zones in the Sun, falling sharply to zero at the exterior (this ignores the external dipole field of the Sun). The strength of the magnetic field outside the resonance region is unimportant in the evolution, so assuming a uniform value interior to the Sun is a good approximation. If the real profile of $B(r)$ is more complicated, as is almost certainly the case, the value of B should be thought of as that at resonance $B(r_{\mathrm{res}})$.

The evolution in the interior was performed using a Runge-Kutta algorithm with adaptive step size control [16] in double precision arithmetic. On order of 10^5 steps were taken for the higher mass gaps, the neutrinos being evolved from 3 full width at half maximum (FWHM) before the resonance [17]

$$\sqrt{2}G_F N_e|_{\mathrm{res}} = \frac{\Delta m^2}{2E}\cos(2\theta) \tag{5}$$

to the edge of the Sun. Since the major effect in the evolution is the resonant conversion, neutrino evolution before the resonance is unimportant. We found that starting the evolution just before the resonance reproduced the probability at the edge of the Sun to within 0.1% of the result obtained by starting at $R = 0$, but gave a substantial saving in CPU time.

In the exterior of the Sun, where the magnetic field is assumed to be zero, the neutrino and antineutrino sectors decouple and the vacuum oscillations can be computed using standard analytic formulas (see [17]). Since each detector signal averages over a period of at least two months (though not necessarily weighted times evenly) we modeled the motion of the Earth in a simple way by averaging the vacuum oscillations over an Earth-Sun distance of $d(1-e/2)$ to $d(1+e/2)$, where the semimajor axis is $d = 1.496\times 10^8$ km and the eccentricity of the Earth's orbit is $e = 0.0167$. This corresponds to the variation in the Earth-Sun distance over three months. Although in reality the average Earth-Sun distance depends on the time of year that the data was taken, the principal effect of averaging is to remove the rapid oscillation of the probabilities for the oscillation lengths of interest here. Thus the results are almost independent of the phase of the Earth in its orbital ellipse.

The general form of the propagation matrix for neutrinos allows for the conversion of electron neutrinos into muon neutrinos and also into muon and electron antineutrinos. The latter conversion can occur in two steps, either by a magnetic moment induced oscillation followed by an MSW-type oscillation, or the reverse. Assuming initially electron neutrinos are emitted, the probability P_i of finding each of the four species at the Earth was computed for a grid of the four parameters. For the continuum spectra we calculated the probabilities for 30 energies ranging from 0.5 to 15 MeV in 0.5 MeV steps, and we also calculated the probabilities at 0.862 MeV and 1.442 MeV corresponding to the ^{7}Be and *pep* neutrino lines respectively. The mass gap, Δm^2, ranged from 10^{-5} to 10^{-8} eV^2; for higher mass gaps the Zeeman energy plays

no role and pure MSW and/or vacuum mixing results. This case has been well studied and the higher mass gaps in the so-called "adiabatic regime" may already be ruled out by experiment [2]. The vacuum mixing angle, $\sin^2(2\theta)$, ranged from 0.01 to 1.00 and the Zeeman energies, μB, from 0 to $5\times10^{-10}\mu_B$ kG. The best limit on neutrino transition moments is astrophysical, coming from the luminosity of red giant stars before and after the He flash [15],

$$\mu < 3\times10^{-12}\mu_B(3\sigma) \tag{6}$$

and the best lab limits (from $\bar{\nu}_e$-e scattering) are [18]

$$|\kappa_e| < 4\times10^{-10}, \quad |\kappa_\mu| < 10^{-9}, \quad \mu_i = \kappa_i\mu_B\ , \tag{7}$$

so the larger Zeeman energies require enormous fields in the solar interior.

The expected event rates in the detectors were calculated by convolving the SSM neutrino fluxes (taken from Tables 6.3 and 6.5 of [1]) and known neutrino cross sections with published detector efficiencies [1,12,19].

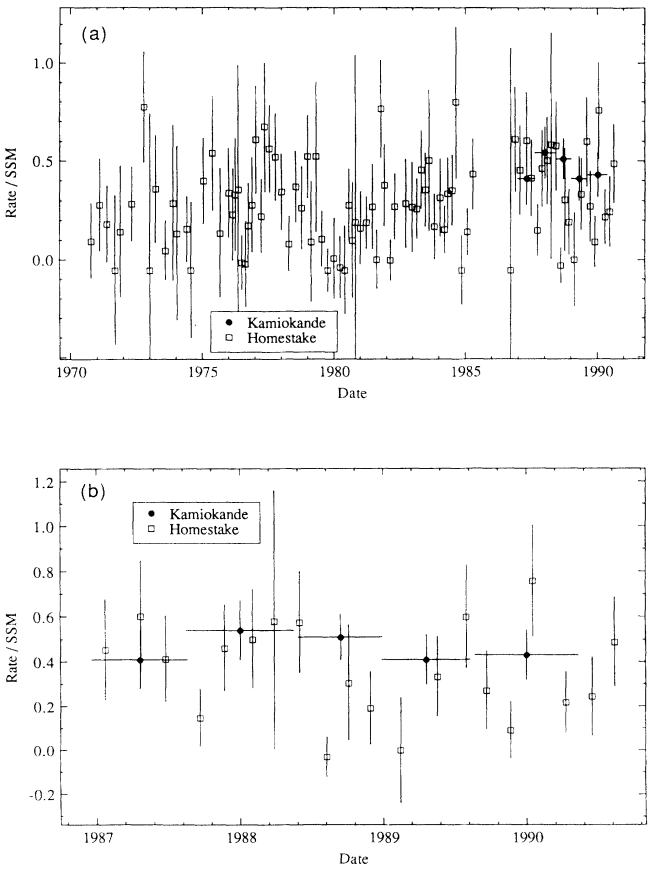

FIG. 1. Shown in (a) is the complete Homestake and Kamiokande data set used in this analysis, with neutrino signal shown as a fraction of that predicted in the standard solar model. Error bars for the Cl data are discussed in the text. In (b) the subset of the sample containing the data obtained concurrently by the two detectors is shown.

III. THE DATA

The 90 Homestake data points between the years 1970 and 1991 were obtained with about two months of integration time per point. The time shown for each Homestake data point in Fig. 1 is the mean time of production of the radioactive argon atoms (see [1] for a description). For each point the experiment reported an upper limit on the production rate, a lower limit on the rate, and the mean value of the rate (which could be zero), all determined by a maximum-likelihood fit to the data [20]. The errors about the mean were generally symmetric, except in the case where the lower limit would have become negative, in which case the reported error bars were quoted as one-half the difference between the upper limit and zero, and were thus sometimes artificially small. This suppression of the errors would artificially increase the weighting of these points in any fit to the data. In order to remove this effect, we utilized fully symmetric error bars on all points. The size of 1σ error bars was fixed to be the difference between the reported upper limit and the mean value for each point. It has been *calculated* that 0.08 ± 0.03 argon atoms/day are produced [1] by the (muon-induced) background. In determining the average Homestake signal it is appropriate to subtract this background *after* the average Ar rate has been computed from the total data set, and add errors in quadrature. When performing a point by point fit of theory to the data, however, it is appropriate to subtract this background from each data point and add its uncertainty to the rate uncertainty for each point in quadrature.[1] This has the effect that the central value of some points can become negative, although the 1σ upper limit is of course always positive, giving a limit on the rate. Figure 1 displays the values divided by the standard solar model (SSM) predicted rate. Because of the unusually small errors on many of the points with small rates, the treatment of errors in the Homestake experiment has been an issue of some debate. In particular the "error" determined by the maximum-likelihood fit is not a Gaussian 1σ error for points with small numbers of counts ($N \leq 5$) and the use of a χ^2 analysis will not weight these points correctly (see, e.g., [21]). To consider the effect of this, for the analysis of the nonstandard solar models and the MSW neutrino model, we also used the method of [21] to analyze the Homestake data, while still using χ^2 for the Kamiokande data.

[1]The average rate (which converts to 0.26 ± 0.04 SSM) quoted by the Homestake group comes from a maximum-likelihood fit of $N=61$ runs to a constant background plus one decaying species. The division of the counts into (counter) background and signal is different if the runs are analyzed separately or collectively, the (counter) background in a run by run analysis being quite variable. We calculate our average rate as the average of the values quoted per run, for $N=90$ runs. Note that 0.26 is bracketed by our weighted and unweighted values (listed in Table I). The larger error, 0.04, is consistent with the smaller number of runs analyzed by the Homestake group.

TABLE I. Average values for solar neutrino data.

Experiment	Averaging method	Average
Kamiokande:		0.4600±0.0781
Homestake:	20-yr weighted:	0.2153±0.0284
	20-yr unweighted:	0.2799±0.0309
	Concurrent weighted:	0.2475±0.0436
	Concurrent unweighted:	0.3602±0.0528

The Kamiokande data are more straightforward. Over the period 1987–1990, five data points have been obtained, based on real-time measurements of the directional solar neutrino signal, averaged over a period of several months. These data points, along with errors, were presented as a fraction of the rate predicted by the SSM [2], and, as shown in Fig. 1, were used directly in this analysis.

Finally, we decided not to additionally weight the Kamiokande and Cl data points in terms of the length of the measuring interval associated with each point. In the first place, longer runs in the Cl experiment do not mean more data. Because the produced Ar atoms decay with a 35 day half-life they will eventually reach an equilibrium abundance after several months exposure. Secondly, the small error bars on the Kamiokande data points presumably reflect the longer exposure times for each point in this experiment, and thus measuring time will in this case naturally be taken into account in any weighting by errors of the data.

IV. ANALYSIS

In an effort to determine how the current solar neutrino data constrains the various possible models discussed in Sec. II, we compared the predicted signals in both detectors to the data by means of a χ^2 goodness-of-fit procedure. For each model we computed the predicted signal over a range of model parameters, and for each combination calculated the value of χ^2 for the signal compared to the data. We then examined the parameter space for χ^2 values corresponding to confidence levels of 68% and 95%.

The different models we considered are (a) nonstandard solar model B flux reduction; (b) nonstandard solar model (B+Be) flux reduction; (c) neutrino mass model (no magnetic moments, constant flux); (d) neutrino mass model (with magnetic moments, variable flux).

In models (a) and (b) we included all neutrino sources. We allowed the overall normalization of the B and Be spectra to vary between 0 and 100% of the SSM value, keeping the shape of the spectrum fixed. In case (b) the Be and B fluxes were reduced by a common amount to allow maximal reduction in the neutrino signal (if the fluxes are reduced because of a lowering of the central solar temperature then Be will be reduced by a factor of $\sim\kappa^{8/18}$ for a B reduction by κ. Thus reducing Be by κ is optimistic and allows a better fit to "low" data). In case (c), each combination of the neutrino mass-squared difference and vacuum mixing angle produced a constant fit to each of the detector signals. In case (d), in addition to these parameters, the quantity μB was assumed to have the form $\mu B = A + Cf(t)$. In this case $f(t)$ was set to either $\cos(\phi + kt)$, where ϕ and k were determined from sunspot data, or to a sawtooth function of unit amplitude with a net period equal to the solar cycle and the position of the cusp given by time τ. This latter model was chosen based on an earlier suggestion by Bahcall and Press [11] that the neutrino time variation could be well described by such a function. We considered $\tau = 8.05$ years, based on their fit to the Ar data, and $\tau = 6.65$ years based on their fit to sunspot data. Thus in case (d) there are two additional parameters A and C involved. The translation of χ^2 values into confidence levels depends upon number of degrees of freedom. In determining the goodness of fit of models (a), (b), and (c) with various sets of parameters, the number of degrees of freedom was set equal to the number of data points, since the model predictions are fixed once the parameters are fixed, and no parameter in this test is minimized to fit the data. In model (d) the number of degrees of freedom was reduced by two since A and C were fit to the data before goodness of fit was evaluated.

Our results are displayed in Tables II and III and Figs. 2–7. The tables list the "best fit" (i.e., smallest χ^2) model

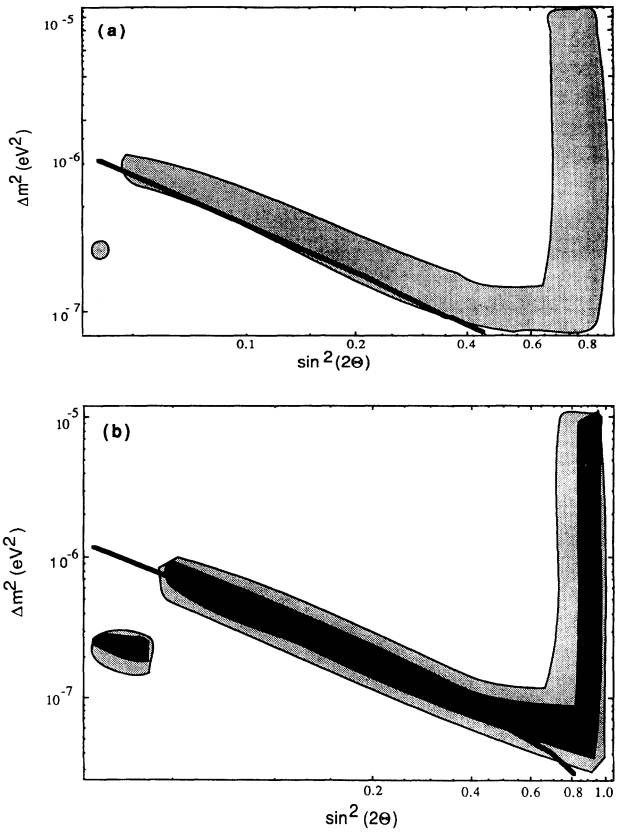

FIG. 2. Those regions in the MSW parameter space (mass-squared difference and mixing angle) which are allowed by the 3-yr concurrent data sample at the 95% confidence levels based on a comparison to (a) all the weighted concurrent data and (b) the unweighted averages of the two concurrent data sets are shown. The line shows the solar neutrino problem "solution" described by Bahcall and Bethe.

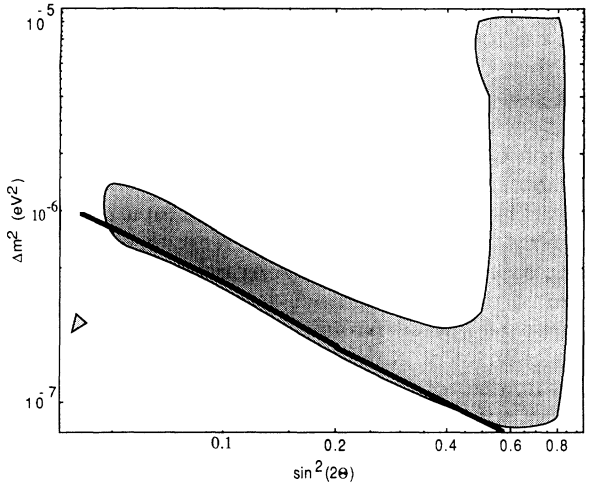

FIG. 3. Those regions in the MSW parameter space (mass-squared difference and mixing angle) which are allowed by the full 20-yr weighted data.

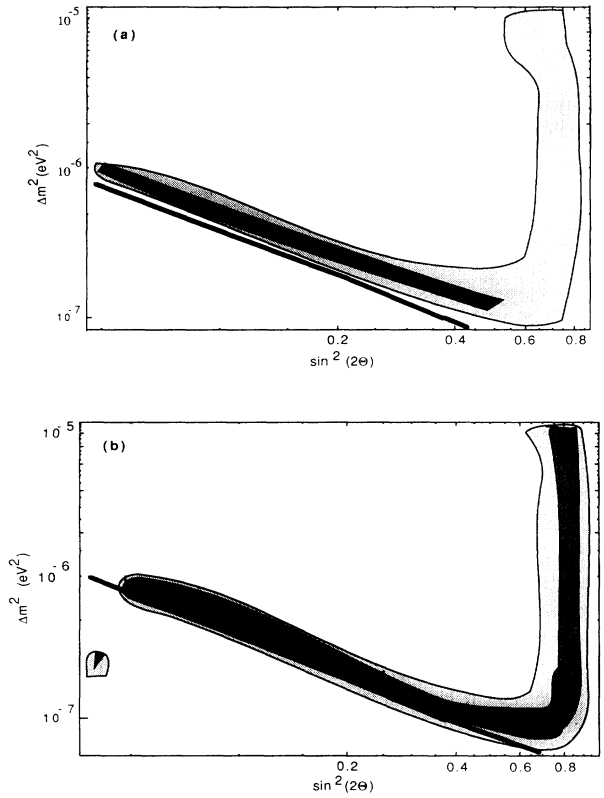

FIG. 4. Same as the last figure, except based on (a) the weighted average signals and (b) the unweighted average signals.

parameters along with degrees of freedom[2] (DF) for fits to (i) the concurrent 3-yr data, and the averaged 3-yr data, and (ii) the complete 20-yr data set, and the averaged 20-yr data. We do not place much significance on the actual value of the best fit parameters, rather we would emphasize the regions in $\Delta m^2 - \sin^2(2\theta)$ space for which the model fits the data at a given confidence level.

Let us review the fits to each of the data sets in turn.

(i) *Concurrent data set.* In spite the apparent similarity of the two signals during this period, the simplest apparent resolution of the solar neutrino problem, that obtained by reducing the B neutrino flux alone, is ruled out at greater than the 4σ level based on a comparison with the weighted data points (including a Be reduction by the same amount allows a fit at the 3σ level). This discrepancy is because the small error bars on the low Homestake points heavily skew any fit. The mean value of the Homestake data during this period arises from 0.25 to 0.36 of the SSM prediction if each point is equally weighted and the fit to a nonstandard solar model improves dramatically. In this case, if the SSM B flux is reduced by a constant factor, the fit to the unweighted averages is acceptable over a small range at the 99% confidence level. Whether or not to ignore the heavy weighting of the apparent anomalously low Cl data points therefore becomes an important issue if one is to claim that nonstandard solar models are ruled out by the combination of Cl and Kamiokande data, at least during the period in which the data was taken concurrently. If the procedure of [21] is used, the nonstandard solar model just fits the concurrent data at the 99% confidence level,[3] with the favored boron flux reduction at 37% of the SSM.

If no model fits the complete fully weighted concurrent data sets, this would provide strong evidence in favor of the assumption that the jitter in the Cl signal precludes its use directly in constraining models, and might provide motivation for ignoring the quoted error bars on the data. As can be seen, however, all the models with neutrino masses, including those with a time variability, provide reasonable fits to the data (at 95% confidence level). The range of fit of the MSW model to this concurrent sample is shown in Fig. 2(a), along with the claimed fit to the 20-yr averaged data by Bahcall and Bethe [16] (solid line). We see that the Bahcall and Bethe line passes through the arm of the 95% confidence level region. If the unweighted averages of the Homestake data sets and the Kamiokande average rate are compared to the MSW prediction, the allowed regions are shown in Fig. 2(b). Notice that the fit to the unweighted average is good at the 68% level over a range of parameters and the 68% region coincides with the Bahcall and Bethe best fit line. An al-

[2]Note the number of degrees of freedom to be used for a goodness of fit and the number quoted for a "best fit" are not the same, the latter being smaller by the number of parameters varied in the fit.

[3]The procedure of [21] makes use of the likelihood ratio test in which the test statistic is χ^2 distributed in the limit of a large number of data points. In applying this test to the concurrent Homestake data we should bear in mind that there are only 20 data points.

TABLE II. Neutrino data χ^2 fits and Ga predictions.

Model	χ^2 (DF)	Parameters[a]	Ga (68%)	Ga (95%)
		Concurrent Data:		
MSW	32.6(23)	1.58,0.25,—,—		5–56
Cosine	30.9(21)	1.26,0.10,2.3,2.3		5–66
Sawtooth (6.65)	31.7(21)	0.25,0.20,2.0,2.0		5–66
Sawtooth (8.05)	31.0(21)	0.16,0.45,2.4,2.4		5–66
Cos (20-yr)	31.7(23)	1.58,0.20		
Saw (20-yr, 6.65)	32.1(23)	1.58,0.15		
Saw (20-yr, 8.05)	31.4(23)	1.26,0.10		
		Concurrent Data (averages):		
MSW (weighted)	0.76(0)	1.26,0.35,—,—	6–56	5–56
MSW (unweighted)	0.002(0)	0.79,0.90,—,—	6–57	6–57
		All Data:		
MSW	101(93)	2.51,0.20,—,—		4–58
Cosine	99.7(91)	3.16,0.15,1.1,1.1	8–12	4–58
Sawtooth (6.65)	97.8(91)	1.26,0.10,1.8,1.8	7–20	5–66
Sawtooth (8.05)	97.4(91)	1.26,0.05,2.0,2.0	5–27	5–66
		All Data (averages):		
MSW (weighted)	1.64(0)	5.01,0.10,—,—	5–20	5–55
MSW (unweighted)	0.15(0)	2.51,0.04,—,—	6–56	6–56

[a]Parameters: $\Delta m^2/10^{-7}$ eV^2, $\sin^2(2\theta)$, $A,B(/10^{-10}\mu_B$ kG), for Zeeman energy $= A + B[\cos(t)$ or saw $(t)]$.

most identical region is obtained for the fit to the weighted averages of the data, suggesting the poorer fit in the case of the individual points is due to "jitter" in the data. If the analysis is done using the method of [21], the MSW model still fits, though the goodness of fit is slightly worse than for the case of the straightforward χ^2 fit.

We now switch to the time-dependent fits, involving a nonzero transition magnetic moment. The "best fit" magnetic field peak Zeeman energy has a value of $4.6\times10^{-10}\mu_B$ kG for the cosine and $4-5\times10^{-10}\mu_B$ kG for the sawtooth fits, which are essentially as good as the MSW fits. Because the 20-yr data provides more compelling evidence of time variability, we also investigated the goodness of fit of the 20-yr "best fit" parameters to the 3-yr concurrent set in the time-varying models. The "best fit" values differ somewhat from the best fit to the 3-yr data, but they are still comparably good. This indi-

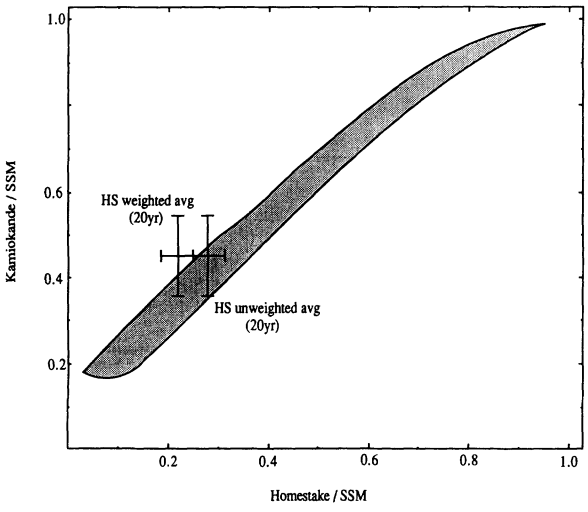

FIG. 5. MSW predictions for Homestake and Kamiokande experiments and experimental rates.

TABLE III. Nonstandard solar model χ^2 fits and Ga predictions.

Model	χ^2	Flux reduction	Ga
	Concurrent Data:		
B	67.5	0.25 of SMM	122
B+Be	49.4	0.30 of SSM	98
	Concurrent Data (averages):		
B (weighted)	20.3	0.18 of SSM	121
B+Be (weighted)	9.74	0.25 of SSM	96
B (unweighted)	7.73	0.30 of SSM	122
B+Be (unweighted)	2.78	0.36 of SSM	101
	All Data:		
B	166	0.09 of SSM	119
B+Be	131	0.20 of SSM	93
	All Data (averages):		
B (weighted)	30.4	0.07 of SSM	119
B+Be (weighted)	14.6	0.18 of SSM	93
B (unweighted)	20.0	0.15 of SSM	120
B+Be (unweighted)	8.63	0.25 of SSM	96

cates that there is no evidence from the concurrent data against the same time variation inferred from the 20-yr Cl sample, although the above discussion makes it clear that the concurrent data are also consistent with a constant rate.

(ii) *20-yr data set.* A nonstandard solar model does not fit the full data much worse or much better than the 3-yr data. The disagreement with the complete weighted data sample, allowing only the B flux to be reduced (in this case to 0.1 SSM), is still at $\approx 4.5\sigma$. Note, however, that now the disagreement with the unweighted average rate (requiring a flux reduction to 0.15 SSM) is comparably bad. Allowing the Be flux to change as well reduces the disagreement, but the fit to the unweighted average in this case is at best only marginal (99% confidence level). The procedure of [21] decreases the goodness of fit dramatically, with the best fit (at 20% of the SSM boron flux) ruled out at $> 5\sigma$.

The MSW model fit to the 20-yr data is shown in Figs. 3 and 4. Notice the line of best fit is shifted slightly from the Bahcall and Bethe line due to the inclusion of the latest Homestake data but the fit is still good at the 95% confidence level. The fits to the weighted and unweighted averages are good (better than 68%) as one might expect. If the method of [21] is used to compute the χ^2, thus taking account of the Poisson statistics of the low points, the best fit is only acceptable at the $\approx 5\sigma$ level. The fact that both the nonstandard solar model and MSW fits, in which the prediction is a constant, are worse using the method of [21] than using a normal χ^2 procedure suggests that this latter method is much more sensitive to "jitter" in the data.

Since it is perhaps the simplest and most elegant of the proposed neutrino based "solutions" to the solar neutrino problem, we feel the MSW model deserves a closer inspection. In this regard we have developed a new way of presenting the comparison between theory and observation. For the 680 $(\Delta m^2, \sin^2 2\theta)$ parameter pairs we calculated in our study, we display in Fig. 5 a plot of the MSW predictions for Homestake vs Kamiokande. While *a priori* one might expect such a plot to "fill" much of the plane, one can see that the allowed region is in fact a narrow band passing from bottom left to top right. This behavior is due to the fact that high energy ^{8}B electron neutrinos make up most of the signal for both detectors, leading to a strong correlation in the signals for an energy-dependent ν_e flux reduction. [We thus expect that adding the neglected contributions from ^{15}O and ^{3}He$+p$ (hep) neutrinos to the Homestake signal will broaden this band slightly.] Still, the narrowness of the band is a surprising indication of the strong constraints on the predictions of the MSW solution. Also shown in

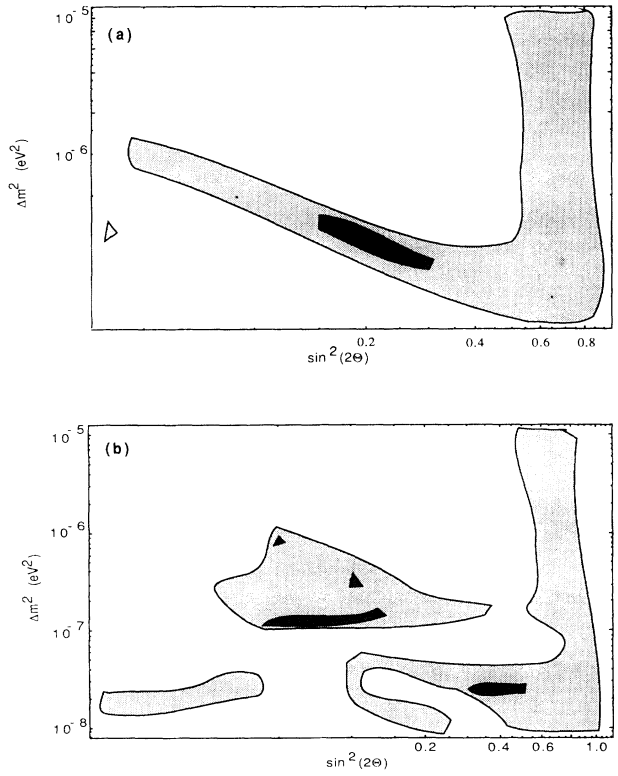

FIG. 6. Those regions in $\Delta m^2 - \sin^2 2\theta$ space which are allowed at the 68% and 95% confidence levels for nonzero transition magnetic moments based on the 20-yr weighted data sample, when the Zeeman energy is fixed to its "best fit" value, with time dependence: (a) $[1.1\times10^{-10}+1.1\times10^{-10}\cos(f+kt)]\mu_B$ kG, (b) $[2\times10^{-10}+2\times10^{-10}\mathrm{saw}(t,\tau=8.05)]\mu_B$ kG.

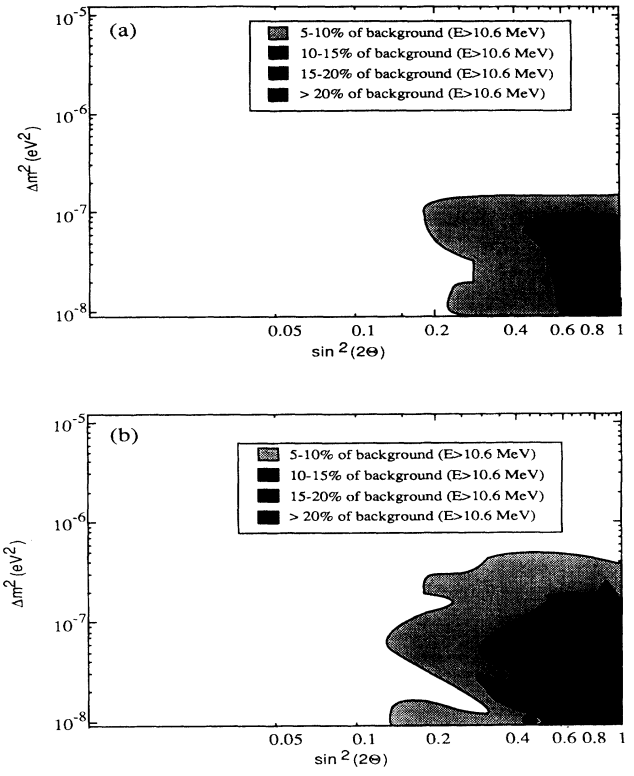

FIG. 7. The predicted electron antineutrino signal in Kamiokande as a fraction of the observed background for incident antineutrinos of energy > 10.6 MeV, for resonant spin conversion models, if the Zeeman energy in the Sun has value: (a) $2\times10^{-10}\mu_B$ kG and (b) $5\times10^{-10}\mu_B$ kG are shown as a function of Δm^2 and $\sin^2(2\theta)$.

Fig. 5 are the averages of the actual rates seen in the detectors. In this way one can obtain a clear and immediate graphical picture of how well the MSW solution as a whole can reproduce the observed averages. As can be seen, the fair overlap between (the constrained) theoretical phase space and the observations is suggestive. More work on this approach is contained in [14].

The low points in the pre-1987 sample can be well accommodated, as has been previously noticed, by a time-varying neutrino signal. In addition, as stressed earlier, resonant spin-flavor transitions also allow "arbitrary" Kamiokande time variation for a given variability in the Cl data. As expected, therefore, we find that the complete data sample can be well fit over a wide range of parameter space by a time-varying magnetic field coupled with a large neutrino transition magnetic moment. Shown in Figs. 6(a) and 6(b) are the regions of mass-mixing angle space allowed at the 68% and 95% confidence levels when the magnetic field time variation is fixed at the value which provides the minimal χ^2 fit to the data for a (a) cosine or (b) sawtooth time dependence. (The actual region of parameter space allowed in this case is a four-dimensional space in mass, mixing angle, and magnetic field time variation—difficult to draw, but whose boundary in the extreme limit of zero magnetic field splitting would reduce to the MSW plot already presented.) The cosine fit to the data at this optimum magnetic field value is obviously better than the zero field MSW fit, while the sawtooth fit is even broader, and slightly better than the cosine fit at the optimum magnetic field value.

The apparent jitter and/or the occurrence of anomalously low data points in the Cl data sample, which dominates over the Kamiokande sample in the 20-yr fits (by about 4 to 1 in the χ^2 determinations), cannot be dismissed based purely on statistical grounds alone. We have investigated whether one might be forced to ignore or rescale the error bars in order to reduce this effect by examining the variance of both the weighted and unweighted Cl 20-yr samples. The mean value of the Cl signal for the complete 20-yr weighted sample is 1.70 ± 0.22 solar neutrino units (SNU). This is significantly smaller than the unweighted average of 2.21 ± 0.24 SNU. Nevertheless, the χ^2 per degree of freedom for this weighted average is 1.07. This indicates that there is no necessity to rescale errors to account for the variance of the sample from the mean. Alternatively, the unweighted sample has a mean variance per point of 1.7 SNU. This is comparable to the error per point in the weighted sample, indicating again that there is no evidence that the errors are skewed in any way.

Finally we stress a somewhat nonintuitive result. In the 20-yr sample, the Cl data clearly dominates in any fit. One may feel that comparing model predictions to average values may alleviate this problem by treating the two data sets with equal weight. However, the relative errors determined for the Homestake mean values are small enough so that the Homestake result dominates the fit to average values (weighted or unweighted) more than it does a fit to the complete sample. Thus, if the Cl data is suspect, for any reason, using average values rather than the full data set will only exacerbate this problem.

One way in which we might hope to proceed further in distinguishing between models is to examine the predictions for the Ga solar neutrino experiments [SAGE and Gallium Experiment (GALLEX) Collaborations] which are currently beginning to run. Estimates of gallium rates predicted by the models we have considered are summarized in the last two columns of Table II. For a given model, we have computed the range of neutrino rates that would be seen in a Ga-based detector for the region of parameter space not already excluded at the 68% and 95% confidence levels by the present Homestake and Kamiokande data. The time dependence of the predicted gallium rates for the time-dependent models varied widely (including no significant time variation) for equally allowed parameter sets. Thus measuring the time dependence of the rates in gallium detectors might help further constrain these models, although if uncertainties in the data are on the same order as the Cl data, a clear measurement of time dependence is unlikely in the short term. Moreover, an observation of no time variation in the gallium detectors would once again not provide definitive evidence against time variation in the Cl signal. In the context of neutrino-based models then the SAGE result, (20 ± 38) SNU, is perhaps the least enlightening result one could obtain from a theoretical point of view [26].

Kamiokande itself now provides another constraint on resonant spin-flavor conversion models. Electron neutrinos can be converted to electron antineutrinos in the Sun, and these contribute to the isotropic background signal in the Kamiokande detector. Thus, the flat background of isotropic events seen by the Kamiokande detector can place a limit on the flux of electron antineutrinos [9]. Although a careful analysis of the data in this regard has not yet been performed, estimates of the flux of electron antineutrinos for neutrino energies greater than or equal to 10.6 MeV for the time period June 1988 through April 1989 are less than approximately 10% of the expected electron neutrino flux predicted by the SSM [22]. For the models discussed in this paper, the predicted electron antineutrino fluxes ranged from 0% to 30% of the SSM ν_e flux. Figure 7 outlines regions of parameter space excluded for various flux limits, for Zeeman energies of 2.0×10^{-10} and $5.0\times10^{-10}\mu_B$ kG respectively. (Indicative of average and peak Zeeman energy values which appear in the best-fit solutions.) Note that some regions favored by the time-varying models are eliminated by the 10%-of-background cut, but none of the time-varying models are completely eliminated on the basis of this constraint alone. As the energy threshold for the Kamiokande background subtraction is reduced, more of the parameter space for magnetic moment induced oscillations can be probed. However, it is worth noting that our results suggest that none of the present "allowed regions" for the time-varying models would be eliminated even if a background cut at the 5% level were made. It is possible that the SNO heavy water detector may eventually be able to distinguish the antineutrino signal more clearly from the neutrino signal, and thus could further improve these bounds.

V. RESULTS

For convenience we summarize the above analysis and restate the main results.

(1) Nonstandard solar models which result in a reduced boron flux are ruled out, for the concurrent weighted data sample, at the 4σ confidence level. This limit is basically unchanged when the rest of the Cl data are taken into account, though the required flux reduction is more extreme. If the unweighted Cl average signal is utilized instead, this simplest nonstandard solar model fits at the 98% confidence level for the concurrent data sample. In this case, however, the fit to the unweighted average of the full 20-yr sample is *incompatible* at the $\approx 4-5\sigma$ level, due to the low long-term Homestake average. The SAGE results now also appear to argue against this possibility. Inclusion of standard solar model uncertainties are not likely to affect the goodness of fits of these nonstandard models at any significant level.

Our results allow a statistical interpretation of the earlier suggestion by Bahcall and Bethe that nonstandard solar models cannot fit the data.

(2) The MSW neutrino mass solution of the solar neutrino model over much of the range claimed by Bahcall and Bethe fits the concurrent and 20-yr weighted data at only the 95% confidence level. We have no statistical evidence that the error bars in the Cl data are anomalous, but if the unweighted mean is utilized instead, the MSW fits improve significantly. This suggests the jitter in the Homestake data may be the cause of the higher $\chi^2/N_{\rm DF}$. On a Homestake vs Kamiokande plot the MSW prediction appears as a thin band which overlaps the averaged data. In this way, the agreement between theory and averaged data is more easily pictured.

(3) Models with resonant spin-flavor conversion due to a varying magnetic field in the Sun fit the data with a confidence level which is at best comparable to the MSW fits—even for the 3-yr concurrent sample in which no time variation in the Kamiokande signal is obvious. As expected, the time-varying models provide acceptable fits to the complete weighted data set much more broadly than the MSW models do, and in the case of a sawtooth time dependence the best fit is also greatly improved. The maximum Zeeman splitting needed in these cases is rather large, of order $2-5\times 10^{-10}\mu_{\rm B}$ kG.

(4) Most neutrino-based solutions to the solar neutrino problem not excluded at the 95% confidence level predict roughly comparable rates in Ga, between 5 and 65 SNU. Nonstandard solar models which are not excluded predict rates greater than 90 SNU. Hence, Ga can decisively rule out nonstandard solar models, but cannot distinguish well between neutrino-based solutions. Acceptable time-varying models predict a wide range of possible time variation in gallium, including almost no observable variation.

(5) Kamiokande can restrict the allowed parameter range for spin-flavor conversion models, and already rules out Δm^2 in the range $10^{-8}-10^{-7}$ eV^2, for mixing angles greater than $\sin^2(2\theta)\sim 0.3$. This limit comes from the isotropic background in the experiment and will improve with time. The SNO detector might improve these further.

VI. CONCLUSIONS

The Kamiokande experiment can provide a useful check on the Homestake experiment, and the combined data from both experiments during their concurrent running is consistent with a wide variety of models. Unfortunately, however, the specifics of which model and what parameters appear to be favored depend upon how one treats the data, so that no categorical conclusions can yet be made.

Future experiments at Kamiokande and with Ga may not allow much finer distinctions between neutrino-based models to be made, but they could definitively rule out nonstandard solar model based solutions of the solar neutrino problem. At this point, 20 years of experiments have at least firmly established the existence of the solar neutrino problem and pointed to new microphysics as the likely solution. To gain the information necessary to completely resolve this issue it will be necessary to measure the solar neutrino spectrum itself. If neutrino mixing is indeed the cause of the solar neutrino problem then a knowledge of which energies are most suppressed would give us a better handle on the underlying mechanism and parameters (for example in simple MSW mixing, in the regions considered here, lowering Δm^2 for a given mixing angle lowers the threshold energy below which $\nu_e \rightarrow \nu_x$ conversion takes place).

Experiments with this goal in mind (i.e., [23,24]) are important to pursue. In this way, a new window on physics at scales beyond those accessible at present accelerators may be fully explored.

ACKNOWLEDGMENTS

We thank Ken Lande for providing us with the complete sets of chlorine neutrino data and for useful discussions on both the Cl and Ga experiments, and M. Smith for informing us of the work of Filippone. We also thank C. Baltay for useful discussions, P. Langacker for helpful advice on error handling, and D. Gelernter and D. Kaminsky of the Linda group of the Department of Computer Science at Yale for running our evolution code on their complex. E.G. was supported in part by the DOE. The research of L.K. was supported in part by the DOE, the NSF, and the TNRLC. The research of M.W. was supported in part by a grant from the TNRLC.

[1] J. N. Bahccall, *Neutrino Astrophysics* (Cambridge University Press, Cambridge, England, 1989); R. Davis, Jr., in *Proceedings of the Seventh Workshop on Grand Unification,* Toyama, Japan 1986, edited by J. Arafune (World Scientific, Singapore, 1986), p. 237.

[2] K. Hirata *et al.*, Phys. Rev. Lett. **63**, 16 (1989); **65**, 1297 (1990).

[3] A. I. Abazov *et al.*, Phys. Rev. Lett. **67**, 3332 (1991).

[4] L. M. Krauss, Nature **355**, 399 (1992).
[5] S. P. Mikheyev and A. Yu. Smirnov, Yad. Fiz. **42**, 1441 (1985) [Sov. J. Nucl. Phys. **42**, 913 (1985)]; L. Wolfenstein, Phys. Rev. D **17**, 2369 (1987).
[6] J. N. Bahcall and H. A. Bethe, Phys. Rev. Lett. **65**, 2233 (1990).
[7] M. B. Voloshin and M. I. Vysotsky, ITEP Report No. 1, 1986 (unpublished); L. B. Okun, Yad. Fiz. **44**, 847 (1986) [Sov. J. Nucl. Phys. **44**, 546 (1986)]; L. B. Okun, M. B. Voloshin, and M. I. Vysotsky, *ibid.* **44**, 677 (1986) [**44**, 440 (1986)]; Zh. Eksp. Teor. Fiz. **91**, 754 (1986) [Sov. Phys. JETP **64**, 446 (1986)]; A. Cisneros, Astrophys. Space Sci. **10**, 87 (1981).
[8] C. S. Lim and W. J. Marciano, Phys. Rev. D **37**, 1368 (1988).
[9] C. S. Lim *et al.*, Phys. Lett. B **243**, 389 (1990).
[10] Y. Elsworth *et al.*, Nature **347**, 536 (1990).
[11] J. N. Bahcall and W. H. Press, Astrophys. J. **370**, 730 (1991).
[12] L. M. Krauss, Nature **329**, 689 (1987).
[13] J. W. Bieber, D. Seckel, T. Stanev, and G. Steigman, Nature **348**, 408 (1990).
[14] M. White, L. M. Krauss, and E. Gates, Report No. YCTP-P14-92 (unpublished).
[15] G. Raffelt, Phys. Rev. Lett. **64**, 2856 (1990).
[16] W. H. Press, B. P. Flannery, S. A. Teukolsky and W. T. Vetterling, *Numerical Recipes* (Cambridge University Press, Cambridge, England, 1986).
[17] S. P. Rosen and J. M. Gelb, Phys. Rev. D **34**, 969 (1986).
[18] W. Marciano, in *Physics Beyond the Standard Model,* Proceedings of the Conference, Lisbon, Portugal, 1988, edited by G. C. Branco and J. C. Romão [Nucl. Phys. B (Proc. Suppl.) **11**, 5 (1989)].
[19] M. Nakahata, Ph.D. thesis, University of Tokyo.
[20] T. Cleveland, Nucl. Instrum. Methods **214**, 451 (1983).
[21] B. W. Filippone and P. Vogel, Phys. Lett. B **246**, 546 (1990).
[22] R. Barbieri *et al.*, Phys. Lett. B **259**, 119 (1991).
[23] B. Cabrera, L. M. Krauss, and F. Wilczek, Phys. Rev. Lett. **55**, 25 (1985).
[24] L. M. Krauss and F. Wilczek, Phys. Rev. Lett. **55**, 122 (1985); see also J. Bahcall, IAS report, 1991 (unpublished).
[25] See S. L. Glashow and L. M. Krauss, Phys. Lett. B **190**, 199 (1987).
[26] L. M. Krauss, Nature **348**, 403 (1991).

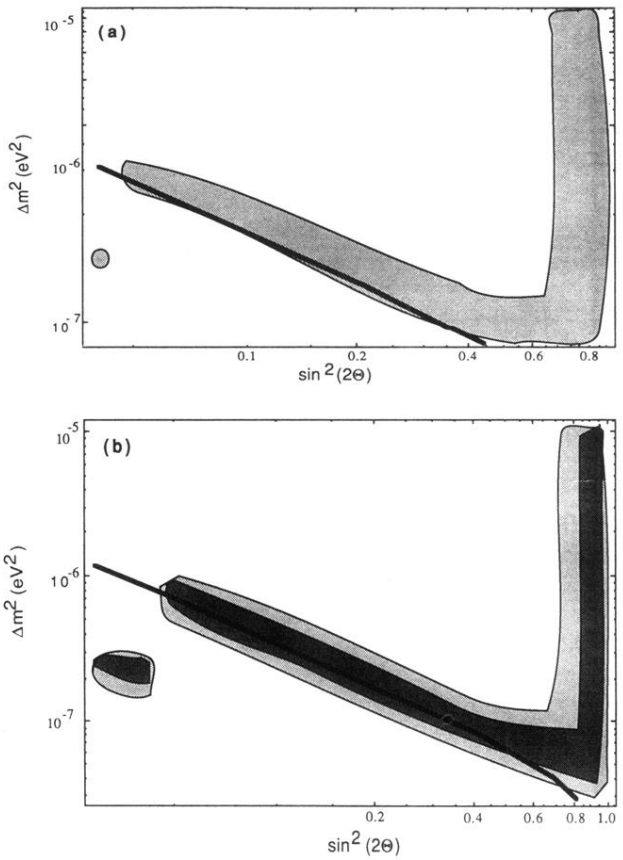

FIG. 2. Those regions in the MSW parameter space (mass-squared difference and mixing angle) which are allowed by the 3-yr concurrent data sample at the 95% confidence levels based on a comparison to (a) all the weighted concurrent data and (b) the unweighted averages of the two concurrent data sets are shown. The line shows the solar neutrino problem "solution" described by Bahcall and Bethe.

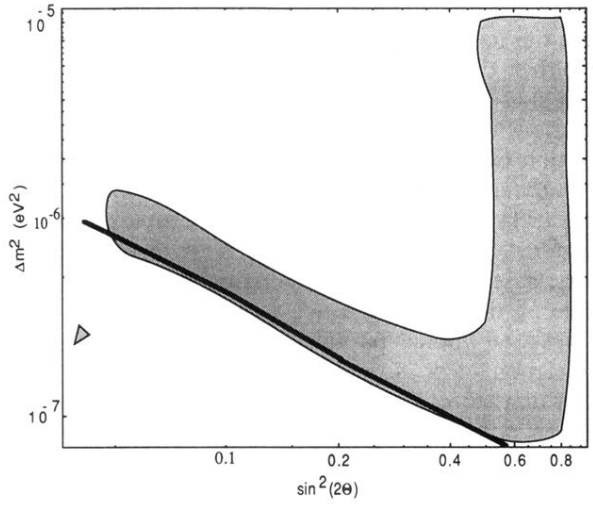

FIG. 3. Those regions in the MSW parameter space (mass-squared difference and mixing angle) which are allowed by the full 20-yr weighted data.

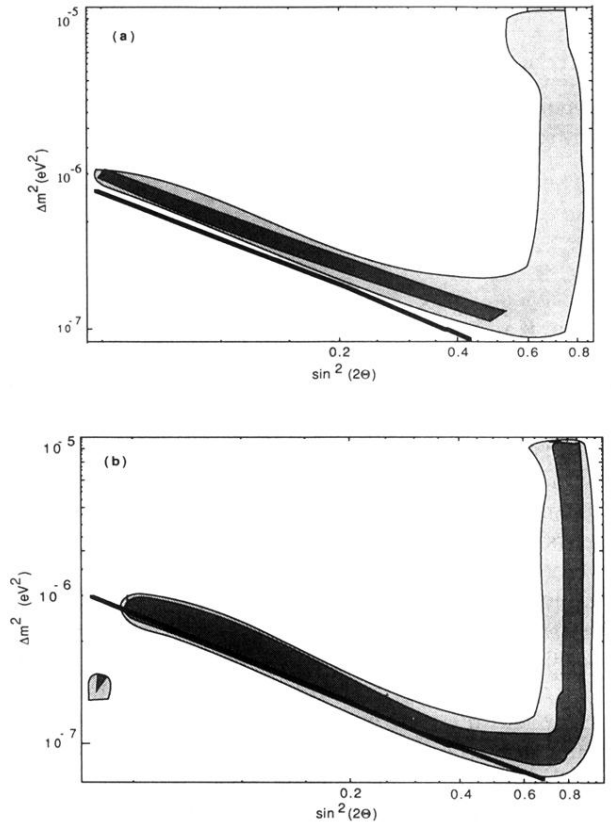

FIG. 4. Same as the last figure, except based on (a) the weighted average signals and (b) the unweighted average signals.

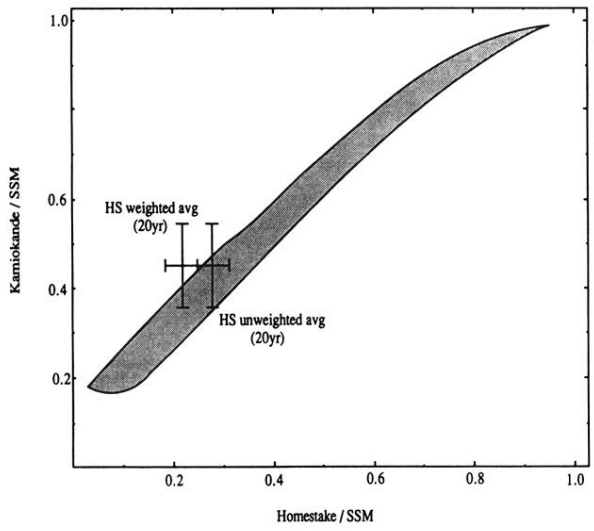

FIG. 5. MSW predictions for Homestake and Kamiokande experiments and experimental rates.

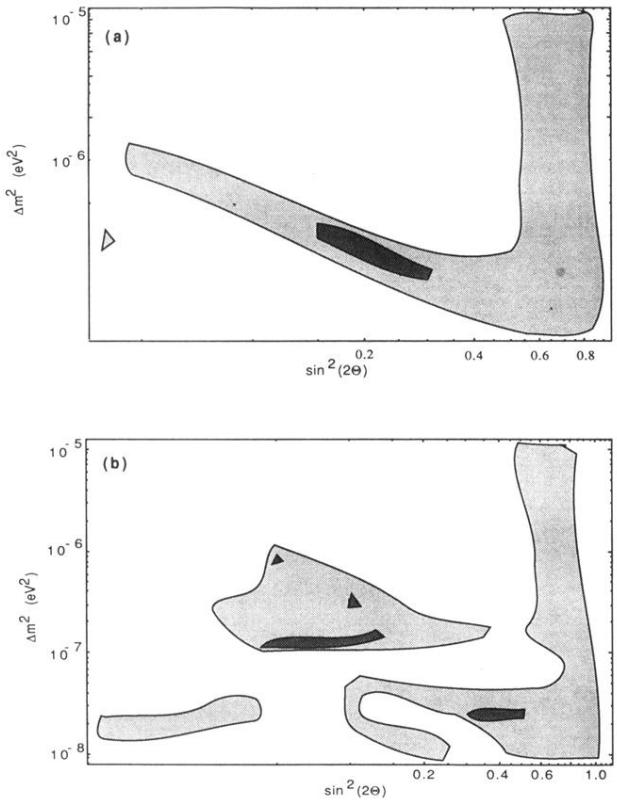

FIG. 6. Those regions in $\Delta m^2 - \sin^2 2\theta$ space which are allowed at the 68% and 95% confidence levels for nonzero transition magnetic moments based on the 20-yr weighted data sample, when the Zeeman energy is fixed to its "best fit" value, with time dependence: (a) $[1.1\times10^{-10}+1.1\times10^{-10}\cos(f+kt)]\mu_B$ kG, (b) $[2\times10^{-10}+2\times10^{-10}\mathrm{saw}(t,\tau=8.05)]\mu_B$ kG.

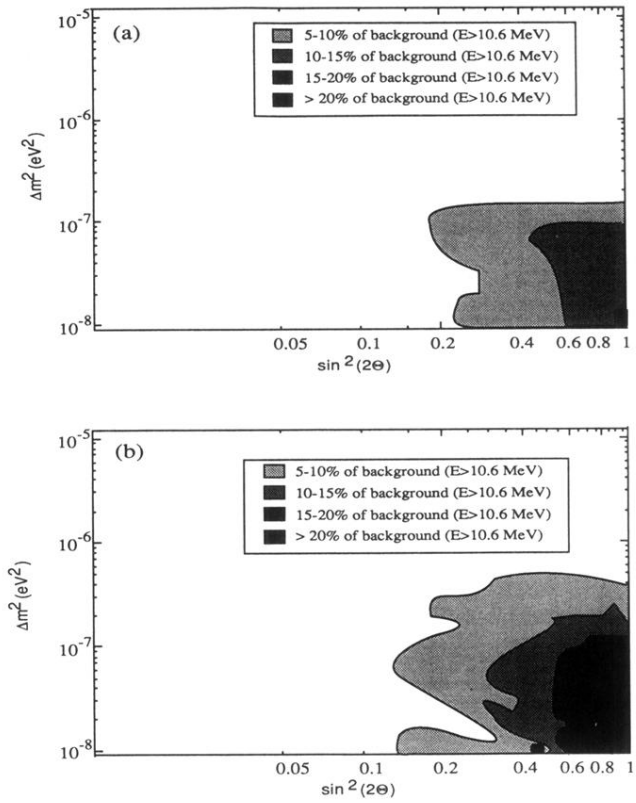

FIG. 7. The predicted electron antineutrino signal in Kamiokande as a fraction of the observed background for incident antineutrinos of energy > 10.6 MeV, for resonant spin conversion models, if the Zeeman energy in the Sun has value: (a) $2\times10^{-10}\mu_B$ kG and (b) $5\times10^{-10}\mu_B$ kG are shown as a function of Δm^2 and $\sin^2(2\theta)$.